Evaluation of saturation in cemented slags with P-wave velocities

Sara Rios[1#], *Nelson* Mica[1], and *António* Viana da Fonseca[1]

[1]*CONSTRUCT-GEO, Department of Civil Engineering, University of Porto, Portugal*
[#]*Corresponding author: sara.rios@fe.up.pt*

ABSTRACT

The application of the circular economy concept to construction engineering and to transportation geotechnics, brings several challenges associated to the use of non-conventional artificial materials. Steel slags can replace natural raw materials, but a thorough mechanical characterisation is needed to assure an adequate behaviour and quality control parameters. The focus of this paper is a mixture of two types of steel slags (a reducing slag and an oxidizing slag) from electric arc furnace steel production. The mixture has cementing properties, mainly due to the reducing slag, being stable in water after compaction. Due to its high stiffness and reduced permeability, the evaluation of the degree of saturation of the mixture using the conventional Skempton parameter B is not very reliable. In this work, P wave velocity measurements in specimens with different cementation levels (given by amount of reducing slag and curing time) and soaked conditions (before and after submersion) were compared. In addition, the elastic shear stiffness evolution with time obtained by S wave velocity measurements demonstrated a clear increase in stiffness with curing time especially in soaked specimens. The aim of the paper is thus to discuss the advantage of P waves to identify full saturation in stiff specimens that harden with time and water. It was found that it is very difficult to evaluate the degree of saturation of a highly cemented specimen, either with the B value or with the P-wave velocities. However, the usual mechanical evaluation by triaxial compression tests is still valid provided that suction is low.

Keywords: ultrasonic transducers; permeability; suction; elastic shear modulus.

1. Introduction

Slags from electric arc furnaces can be distinguished into black or oxidizing steel slags (Electric Arc Furnace -EAF), and white or reducing steel slags (Ladle Slag - LS), where black slags are typically denser than white slags (Geyer 2001). In Portugal, EAF with controlled production have been certified as "Inert Steel Aggregate for Construction", being currently applied in civil engineering works, for instance as aggregate in bituminous or Portland cement concrete. In opposition, the LS has currently no application in construction due to its fine grain size, low strength and high percentage of calcium and magnesium oxides, which can cause expansion problems (Kambole et al. 2017). Varanasi et al. (2019) states that the valorisation of slags is directly linked to the characterization and knowledge of the production process and its behaviour. Although the LS has a similar behaviour to lime, which is already frequently used to stabilise soils, it has not been applied in construction to improve soils or aggregates. This is mainly due to lack of studies and dynamic chemical composition resultant from the industrial process, according to the different temperatures and components that are inserted into the furnace (Aminorroaya et al. 2004).

Since the EAF have reduced percentage of fines (particles smaller than 0.063 mm), larger particles become mostly in contact with each other to distribute the loads, and the fines are not enough to fill the voids between the coarse particles. This results in higher porosities and lower densities when the layer is compacted. For this reason, technical specifications for earthworks usually specify a small percentage of fines in order to obtain a wider grain size distribution curve. To address this requirement EAF have to be milled or mixed with a filler. This filler can be of the same or different origin and is intended to improve the stability or mechanical capacity of the mixture. One possibility is to use the LS for this role.

As currently existing normative and quality control documents related to unbound granular layers for transport infrastructures (e.g., AREMA 2013 and NTG 2015) were developed for natural materials, new materials should be subjected to evaluation of their technical and environmental performance based on laboratory and field tests, so that new design parameters can be provided to ensure the good performance of these alternative materials. For this reason, laboratory procedures need to be adapted to these alternative materials.

This paper addresses some specific issues related to the evaluation of the degree of saturation in specimens made of EAF mixed with LS. Since the envisaged application of this material is for bases and sub-base layers of transport infrastructures, the material is supposed to be unsaturated during most of its lifetime. However, for the lower bound mechanical characterisation of the material it is important to assure low values of suction created during layer flooding.

The assessment of soil full saturation is usually measured by the Skempton pore pressure coefficient (B-value). This coefficient is defined by the Eq. (1), as the ratio between the increment of the isotropic confining pressure ($\Delta\sigma$) with the corresponding increment of pore pressure (Δu) under undrained conditions (Skempton 1954).

$$B = \frac{\Delta u}{\Delta \sigma} \quad (1)$$

Due to the volumetric compressibility of granular media, in fully saturated conditions, the B-value corresponds to $\Delta\sigma \approx \Delta u$, i.e. it is approximately 1. This response corresponds to a combination between the bulk modulus of soil skeleton (K_{sk}) and the bulk modulus of the pore fluid (K_f) descripted by (Skempton 1954).

However, the cementation provided by the LS, which increases the stiffness and reduces permeability, prevents an accurate measurement of B value. When a confining stress is applied to the specimen, its cementing structure sustains the load without transferring it to the pore water pressure.

An alternative way to know if the specimen is saturated is to use P wave velocities (Yang 2002; Valle-Molina and Stokoe 2012). As mentioned by Nishio (1987) and Kokusho (2000) a change in *B*-value between 0.8 and 1 leads to a considerable variation in P-wave velocity and that when the soil voids are filled with water, Vp should be almost equal to the propagation velocity of pure water (1500 m/s).

Yang (2002) proposed a simplified model based on Biot's theory to correlate P wave velocities (Vp) with *B*-value (Eq. (2))

$$Vp = \sqrt{\frac{\frac{4}{3}G_{soil} + \frac{K_{sk}}{1+B}}{(1-n)\rho_{soil} + n\rho_f}} \quad (2)$$

where G_{soil} is the shear modulus of the soil, K_{sk} the bulk modulus of soil skeleton, ρ_{soil} the mass density of the soil, n the porosity of soil, and the ρ_f is the is bulk mass density of the fluid.

This relationship has been applied by other researchers, demonstrating a good adjustment to different experimental results (Kumar and Madhusudhan 2012; Cordeiro et al. 2022).

However, Ishihara et al. (1998, 2001) have found some discrepancy between theoretical prediction and experimental data, particularly for *B*-values between 0.5 and 1. Gu et al. (2021) states that these discrepancies are due to the effect of the type of fluid and gas, the distribution and homogeneity of the included air bubbles, the morphology of soil grains (Astuto et al. 2022) and the size of soil particles (Hakanata and Masuda 2008). The discrepancy between the theory and the experimental data increases as the size of soil particles increases (Astuto et al. 2022).

Bearing this in mind, P wave velocity measurements were performed in mixtures of EAF and LS with varying amounts of LS, creating distinct cementation levels. The paper presents the comparison of P-wave velocities before and after submersion, suction measurements by the paper filter method, as well as the mixture permeability on the flooded specimens. In addition, the elastic shear stiffness evolution with time was obtained by S-wave velocity measurements.

For this purpose, ultrasonic transducers were used due to its easy application in these stiff specimens since they are non-intrusive conversely to bender elements. Also, resonant column tests can be difficult in stiff soil specimens.

Although Rios et al. (2017) demonstrated the great advantage of these transducers in cemented soils to evaluate the stiffness evolution with time, these measurements generally rely on the use of a fixed input frequency, corresponding to the nominal frequency of the transducer. This procedure has shown some limitations when applied to curing materials, i.e. when the stiffness is changing with time (Ferreira et al. 2021). To this end, Ferreira et al. (2021) proposed the use of a wide range of frequencies, from 24 to 200 kHz, in each of the curing periods, instead of a single frequency reading. As a result, an increase in the optimum frequency with curing time was observed, thus demonstrating that the frequency should be adjusted with the increase in stiffness due to curing, generating clearer, more accurate signals. This enhanced procedure was applied in this work.

2. Testing material and procedures

2.1. Material

Fig.1 shows the grain size distribution curves of both slags, showing that EAF has lack of fines, as required by most technical guidelines, such as the Standard Specification for Roadworks (NTG, 2015) from the Australian Department of Infrastructure, to enable an efficient compaction. Table 1 summarises some physical parameters of both materials.

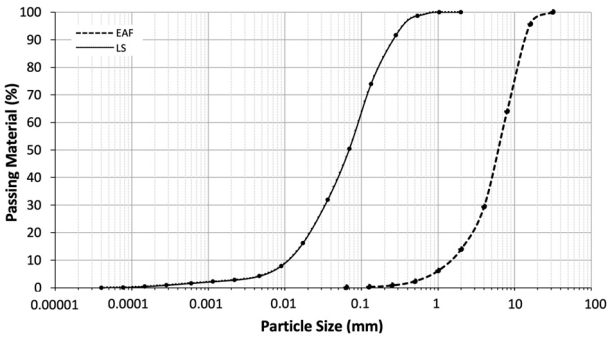

Figure 1. Particle size distribution curves of EAF and LS.

Table 1. Physical parameters of the slags

Parameters	Material	
	EAF	**LS**
Gs	3.83g/cm^3	3.18g/cm^3
D_{max}	9.50mm	2.00mm
D_{50}	4.47mm	0.07mm
Cu	3.79	8.18
Cc	1.13	1.10

In this study, mixtures of EAF with 30%, 40% and 50% of LS were adopted defined as the amount of LS divided by the amount of dry EAF. Fig.2 shows their particle size distribution within the Australian Standard

Specification for Roadworks (NTG 2015) range for sub-base materials.

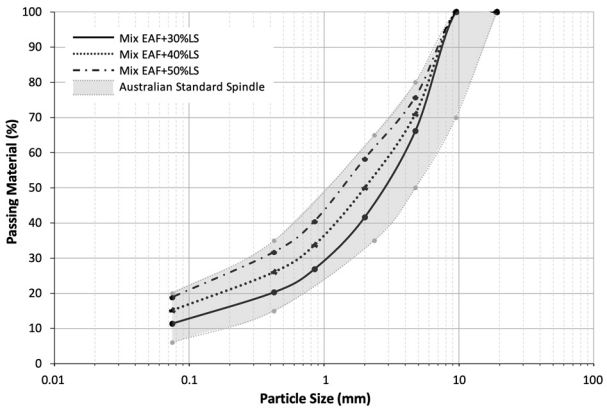

Figure 2. Particle size range of the EAF + LS mix envisaged for the tests in the spindles defined by the Australian standard *(NTG 2015).*

Table 2 summarises the characteristics of the different mixtures indicating for each mixture the % LS, the dry unit weight, the water content and the void ratio. Three unit weights were chosen to perform the tests: 20.5; 21.5 and 22.5kN/m^3 (corresponding to 90%, 94% and 98% of the optimum Standard Proctor value). The water content was fixed for all the specimens corresponding to the optimum value of the Standard Proctor curve.

Table 2. Description of the mixtures of materials under study

Mixture	LS %	Dry unit weight	Water content	Void ratio
EAF+30%LS	30	22.5kN/m^3	12%	0.60
EAF+40%LS	40	22.5kN/m^3	12%	0.59
EAF+50%LS	50	22.5kN/m^3	12%	0.58

2.2. Sample preparation

After weighing the slags, they were mixed until reaching uniform consistency. Water was then added while continuing mixing until a homogeneous paste was created, the quantity of water being based on a target moisture content (Fig.3).

Figure 3. Mixing the material with the optimum water content.

The compaction was carried out in three layers in a cylindrical stainless-steel mould that has been lubricated. Moulds with 50 mm of diameter were used for seismic wave measurements, while moulds with 70 mm of diameter were used for suction and permeability measurements. Both had a height/diameter ratio of 2. Each layer was slightly scratched for better bonding. The mixing and compaction were performed in less than one hour. At least 12 hours after moulding (to prevent swelling) the specimen was extracted from the mould, and its weight and dimensions were measured with accuracies of 0.01g and 0.1mm.

The specimens were tested at several curing times (1, 3, 7, 14, 21 and 28 days) in soaked and non-soaked conditions. Non-soaked specimens were placed in plastic bags to avoid significant variations of moisture content (Fig.4) and they were left to cure in a humid room at 23º±2ºC temperature and 95% relative humidity. Soaked specimens were submerged in water after 1 day of curing and then remained submerged throughout the curing period.

Figure 4. Storage of specimens in cling film.

2.3. Testing equipment and procedures

2.3.1. Seismic wave measurements

Seismic waves propagation velocity was measured using a Pundit Lab ultrasonic testing equipment (Fig.5).

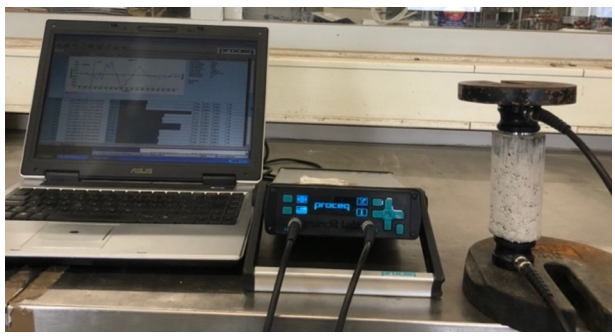

Figure 5. Equipment for carrying out the P-wave and S-wave test – PunditLab.

The measuring set included a pulse waveform generator and data acquisition unit, equipped with an amplifier, directly logged to a PC, using specific software to operate as an oscilloscope. The description of the experimental setup, calibration and measuring procedure is fully described in Rios et al. (2017).

A pair of piezoelectric ultrasonic compression transducers was used for measuring P-wave velocities, with a nominal frequency of 82 kHz and 30 mm in diameter (Fig.6. A). For measuring S-wave velocities, a pair of piezoelectric ultrasonic shear transducers was used with a nominal frequency of 100 kHz and 35 mm in diameter (Fig.6. B).

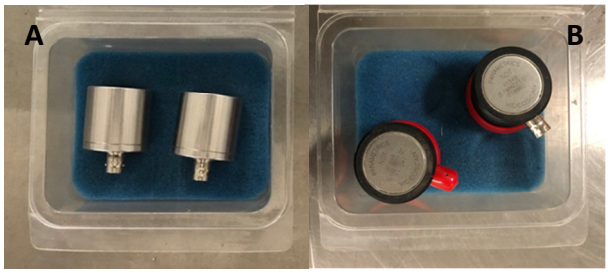

Figure 6. Transducers: A. 82kHz to measure P-waves; B. 100kHz to measure S-waves.

The frequency of the input signal varied between 24, 37, 54, 82 and, on occasion, 150 and 200 kHz, depending on the specimen stiffness as concluded by Ferreira et al. (2021). The propagation time was selected in a time domain procedure based on the first direct arrival of the output wave method (Viana da Fonseca et al. 2009), where the direct measurement of the time interval between the input and output waves assumes the plane wave-fronts and the absence of any reflected or refracted waves.

Measurements were taken along the longitudinal axis of the specimens, with the specimen aligned vertically and the transducers installed on opposite faces (Rios et al. 2017). The transmitter was located at the bottom of the sample, while the receiver was at the top end together with a 1 kg disc to ensure a good contact between the transducers and the specimens. Additionally, ultrasonic gel was used to improve acoustic coupling.

As well-known from the elasticity theory, the shear wave velocities are directly related to the elastic shear modulus (G_0), according to Eq. (3).

$$G_0 = \rho V_S^2 \tag{3}$$

where ρ is the density of the soil

2.3.2. Suction (Filter paper method) and Permeability

A simple and cheap way to estimate the soil suction is the filter paper method based on the principle that when a wet soil is placed in contact with a drier filter paper inside a sealed container, the paper absorbs the water from the soil until both materials equilibrate in suction. Suction can be obtained by the measured water content of the filter paper using a calibration curve. For Whatman No.42 filter paper, suitable for measuring suctions between 0 and 200 kPa, Chandler et al (1992) proposed the following equations (Eq. (4) and Eq. (5)) for the calibration curve:

- If the filter paper water content is higher than 47% (w > 47%):

$$Suction\ (kPa) = 10^{(6.05-2.48\log w)} \tag{4}$$

- If the filter paper water content is lower than 47% (w < 47%):

$$Suction\ (kPa) = 10^{(4.84-0.0622\,w)} \tag{5}$$

The suction was performed on half of the initial specimen with approximately 70mm high and 70mm in diameter.

Although ASTM D5298-94 (ASTM 1998) suggests that filter paper should be oven dried, for these tests air dried filter paper was used directly from the box as suggested by Marinho and Oliveira (2006) to avoid any influence on the absorption characteristics of the filter paper. Pieces of Whatman No.42 filter paper are placed above and below the sample (being previously weighted in a high precision balance with precision of 0.001 g) which is then wrapped in cling film to ensure good contact between the soil and the filter paper. The specimens were placed in a sealed plastic bag and, then placed in a Styrofoam box during the equilibrium time to avoid temperature fluctuations. An equilibrium time of 7 days was considered according to ASTM D5298-94 (ASTM 1998). After this time, the filter paper was removed and its weight was measured in a high precision balance as soon as possible. The specimen was also weighted so that its water content was evaluated and consequently the degree of saturation (S) was obtained.

Permeability tests were performed in a triaxial cell. First a percolation stage was performed during 6 hours with back pressures of 10 kPa at the bottom and 0 kPa at the top, and 20 kPa or cell pressure. Then the pressures were increased to back pressures of 105 kPa at the bottom and 95 kPa at the top, and 110 kPa of cell pressure. These pressures were kept constant until a constant flow rate was obtained, so that permeability could be calculated applying Darcy law.

3. Results

3.1.1. Shear wave velocities

Fig.7 shows, as an example, the S waves output signal obtained on EAF+30%LS mixture, indicating the propagation time recorded in each measurement at 0, 3, 7, 14, 21 and 28 days of curing, using a classical time domain approach (Viana da Fonseca et al. 2009).

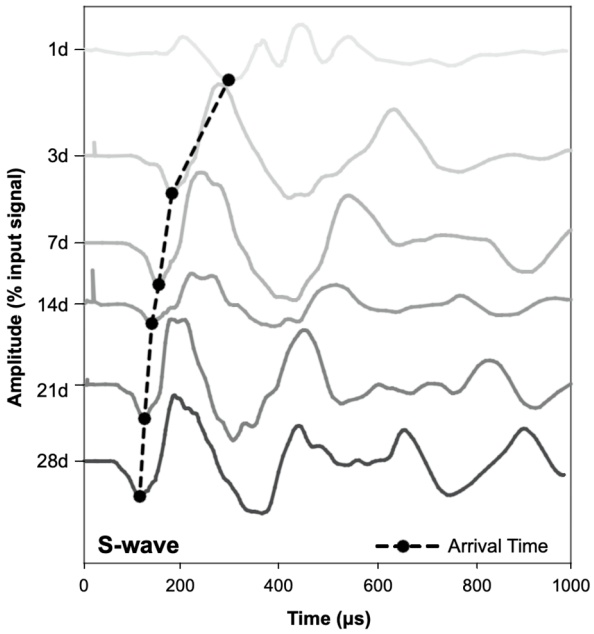

Figure 7. Determination of S-wave propagation time for a mixture of EAF+30%LS.

The identification of S-wave the propagation time corresponds to the first big break downwards (the polarity of the signals was determined during calibration), corresponding to the beginning of a low frequency wave with 24Hz, typical of shear waves.

Note that this a pure shear wave and the flexural mode can be disregarded since the contact between the ultrasound transducer and the specimen is face to face, thus it is unlikely that flexural propagation occurs.

Fig.8 and Fig.9 shows the evolution of the shear wave velocity with curing time for the three mixtures with 30, 40 and 50% of LS up to 28 days. Three specimens were cast for each mixture, identified as EAF+30%LS, EAF+40%LS and EAF+50%LS, and then an average line was drawn to ensure a more accurate comparison.

There is a significant evolution of shear wave velocities with curing time, especially for soaked conditions. In fact, soaking conditions demonstrated to have a very significant influence on shear wave velocities, and consequently, on the material elastic stiffness. This may be due to the calcium hydration present in the LS leading to cementitious compounds that bind the EAF particles increasing the overall stiffness. This is more evident when the LS content is higher, justifying the higher stiffness of EAF+50%LS mixture. Associated to higher shear wave velocities, a higher evolution rate is also observed in the soaked specimens, indicating that the access to water may not be just an acceleration mechanism but also a way to improve the final strength. However, further tests with higher curing periods are needed to clarify this.

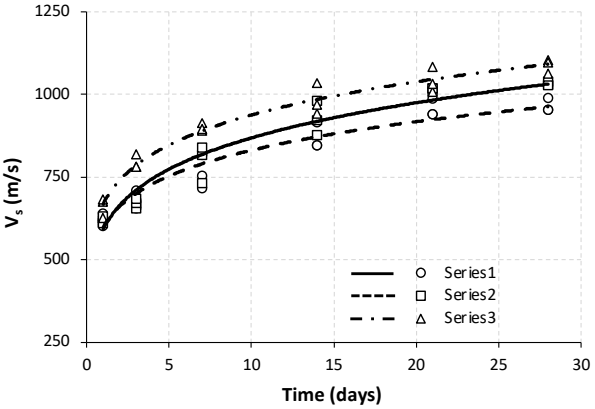

Figure 8. Shear wave velocity evolution with time for soaked condition

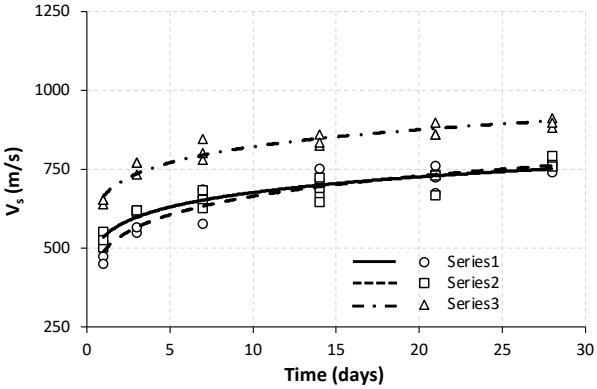

Figure 9. Shear wave velocity evolution with time for non-soaked condition.

3.1.2. Compression wave velocities

Fig.10 illustrates, as example, the determination of the P-wave propagation time for EAF+30%LS, corresponding to the first break of the received wave signal.

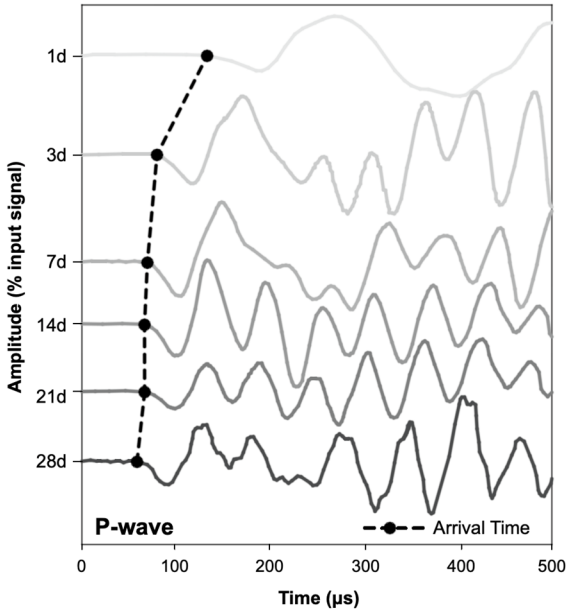

Figure 10. Determination of wave propagation time for a mixture of EAF+30%LS for P-wave

The Vp values obtained for soaked condition ranged from 1256 m/s to 1883 m/s (Fig.11), and for non-soaked condition from 719 m/s to 1636 m/s (Fig.12). It is also interesting to notice that the values of Vp in soaked condition (Fig.11) are practically the same for the three mixtures, indicating that their different stiffnesses has no effect (Fig.12).

It is well known that Vp in water is around 1500 m/s. Therefore, in loose sandy soils which have Vp in unsaturated conditions below 1500 m/s, Vp approaches 1500 m/s when the soil is saturated as the wave propagates much faster through the water than through the soil grains. For this reason, P wave velocities are frequently used to evaluate if the soil is saturated (Valle-Molina and Stokoe, 2012; Cordeiro et al., 2022). This idea seems to be applicable to this particular material, as their Vp in unsoaked conditions is below 1500 m/s. However, Fig.8 and Fig.9 indicate that there is a substantially increase in stiffness when the specimens are placed in water, which means that it is not totally obvious that the P waves will propagate faster through water in a saturated cemented specimen.

Although equation (2) was not developed for this material and may not be totally applicable, it is interesting to notice that B values obtained with that relation are around 0.5, expressing non saturated conditions.

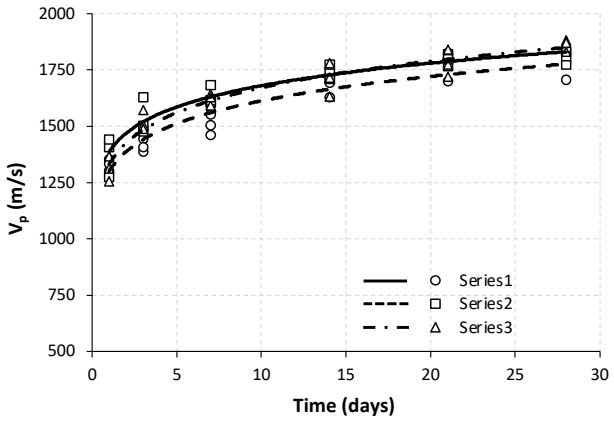

Figure 11. Compressional wave velocity evolution with time for soaked conditions.

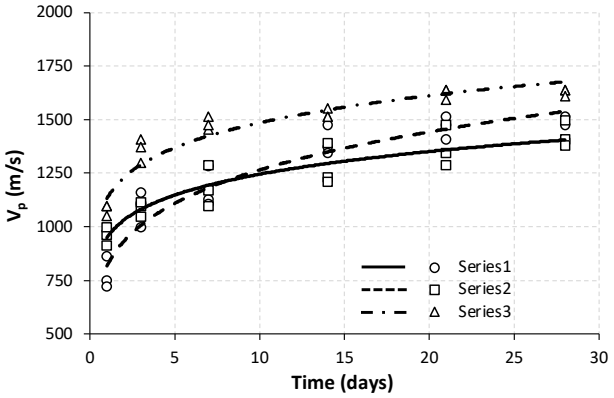

Figure 12. Compressional wave velocity evolution with time for non-soaked conditions.

3.1.3. Poisson ratio

Fig.13 and Fig.14 present Poisson ratio values obtained in the soaked and non-soaked specimens respectively. Fig.14 shows a tendency of Poisson ratio decrease with curing time and LS content, obtaining minimum values of approximately 0.26 and 0.28 for mixtures with 50% and 40% LS at 28 days. These values are typical of highly cemented specimens (Rios et al., 2017). In non-soaked conditions, Fig.13 shows more constant values around 0.3, since the cementation was not enhanced by the contact with water.

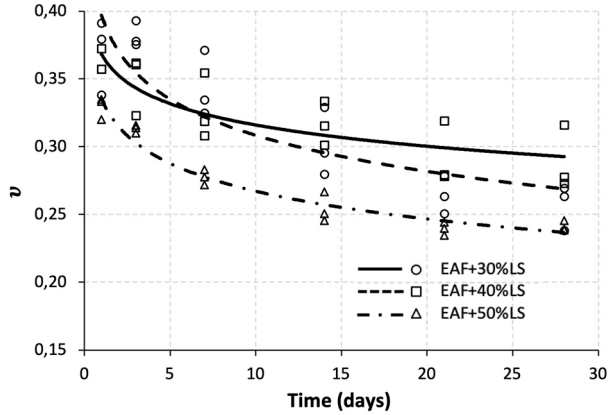

Figure 13. Poisson ratio evolution with time for soaked conditions.

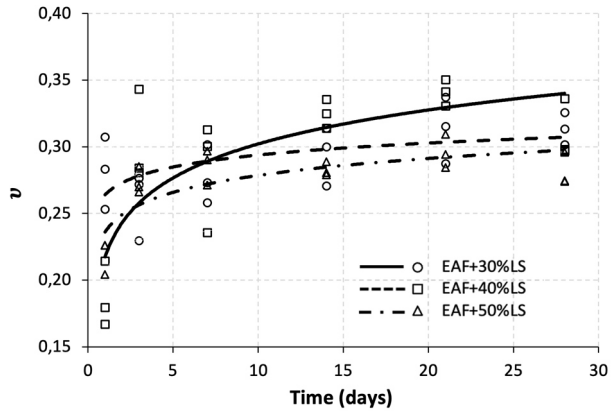

Figure 14. Poisson ratio evolution with time for non-soaked conditions.

However, in any case the Poisson ratio approaches 0.5, which would indicate a P wave propagation through water. This indicates that, either the specimens are not saturated or P waves are not going exclusively by the water due to the high stiffness of the soil skeleton.

3.1.4. Suction and permeability

The permeability values obtained after 1 and 28 days (Fig.15), show that for mixtures of EAF+30%LS, EAF+40%LS and EAF+50%LS, the permeability varies from 1.42×10^{-5} m/s to 7.37×10^{-6} m/s at day 1, and from 6.84×10^{-6} m/s to 1.42×10^{-7} m/s at 28 days, as can be seen on Fig.15. The reduction in permeability at 28 days is a result of cementation, especially in the stiffer mixtures. For the less stiff mixture (EAF+30%LS) permeability reduces to half of its value, while for the stiffer mix (EAF+50%LS) permeability reduces to 2% of the initial value. This demonstrates that permeability reduces significantly with curing time and LS content, as the cemented structure is more closed and the voids are smaller.

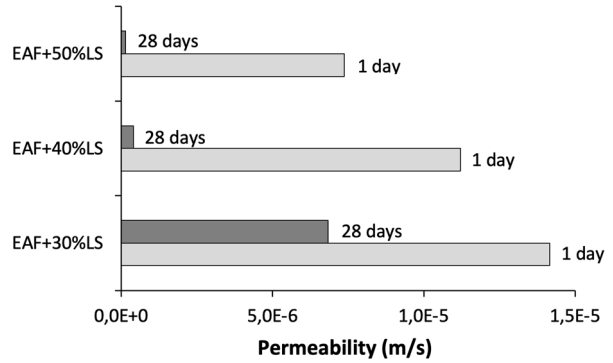

Figure 15. Permeability values at 1 and 28 days.

Analyzing the suction results presented in Fig.16 it becomes clear that suction is higher in the less permeable specimens. This indicates that lower permeability reduces the migration of water to the specimen surface in contact with the filter paper. However, the suction values are quite low and similar between the specimens, which assures that it has an insignificant effect on any strength evaluation.

Moreover, the degree of saturation calculated from the water content of the specimen after the filter paper measurements was around 73.1%.

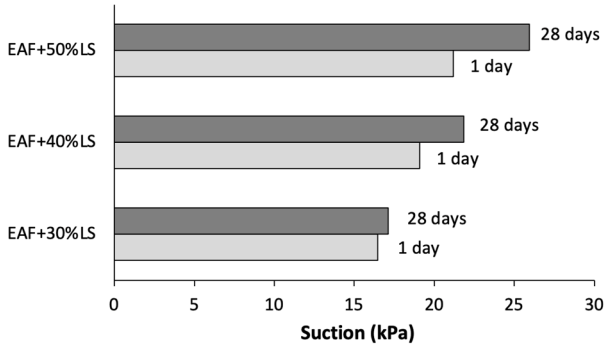

Figure 16. Suction values at 1 and 28 days.

4. Conclusions

Recognizing that Skempton B parameter is not very reliable in very stiff cemented specimens, P wave velocities could be an alternative way to assess full saturation. This paper discusses this issue for a mixture of two different steel slags which tend to cement in contact with water. P wave velocities were higher in soaked conditions in comparison to non-soaked conditions, being as high as 1750 m/s at 28 days. However, Poisson ratio values never got close to 0.5, which would be a sign of P wave propagation through water. So, in spite of very high values of P wave velocities it is possible that the specimens are not fully saturated. The fact observed in Fig.11 that P wave velocities are similar for the different specimens may be explained by a combination of P wave propagation through soil skeleton and water. When the contact bonds are stronger (as it is the case of more cemented specimens), the wave may propagate faster in the soil skeleton, while in the less cemented specimens, the wave may have a higher propagation path through water. The low values of the saturation degree and the low values of B obtained by equation (2), indicate that eventually the specimens are not saturated. Is it possible that a specimen submerged in water for 28 days is not at least 90% saturated? The conclusion of this work is that it is very difficult to assess the saturation degree of a highly cemented specimen (especially if its stiffness increases in water) either with B value or P wave velocities. However, provided that suction is a minor component of the measured strength, the usual mechanical evaluation by triaxial compression tests is still valid. This enables the necessary strength parameters to evaluate the material performance in the support layers of transport infrastructures, even when flooded.

Acknowledgements

The authors would like to thank MEGASA for providing the slag materials as well as information support. Part of the work was conducted in the framework of the TC202 National Committee of the Portuguese Geotechnical Society (SPG) 'Transportation Geotechnics', in association with the International Society for Soil Mechanics and Geotechnical Engineering (ISSMGE-TC202). This work was financially supported by: Base Funding - UIDB/04708/2020 of the CONSTRUCT - Instituto de I&D em Estruturas e Construções - funded by national funds through the FCT/MCTES (PIDDAC). The second author also acknowledges the support of FCT through CEECIND/04583/2017 grant.

References

Aminorroaya, S. E., A. Tohidi, J. Parsi, and B. Zamani. 2004. "Recycling of ladle furnace slags." *2nd International Conference on Process Development in Iron and Steelmaking (SCANMET II)*, no.2: 379-384.

AREMA. 2013. "Manual for Railway Engineering", American Railway Engineering Maintenance-of-way Association, Vol. I to IV, Lanham.

ASTM "D 5298-94 Standard test method for the measurement of soil potential (suction) using filter paper", ASTM International, Annual Book of Standards, Vol. 04.09, West Conshohocken, PA, 1998.

Astuto, G., F. Molina-Gómez, E. Bilotta, A. Viana da Fonseca, and A. Flora. 2022. "Some remarks on the assessment of P-wave velocity in laboratory tests for evaluating the degree of saturation." *Acta Geotechnica*. https://doi.org/10.1007/s11440-022-01610-9

Chandler, R. J., M. S. Crilly, and G. Montgomery-Smith. 1992. "A low cost method of assessing clay desiccation for low rise buildings." *Proc. Institute of Civil Engineering* 92, no.2: 82-89. https://doi.org/10.1680/icien.1992.18771

Cordeiro, D., F. Molina-Gómez, C. Ferreira, S. Rios, and A. Viana da Fonseca. 2022. "Cyclic Liquefaction Resistance of an Alluvial Natural Sand: A Comparison between Fully and Partially Saturated Conditions." *Geotechnics* 2: 1-13. https://doi.org/10.3390/geotechnics2010001

Ferreira, C., S. Rios, N. Cristelo, and A. Viana da Fonseca. 2021. "Evolution of the optimum ultrasonic testing frequency of alkali-activated soil-ash." *Géotechnique Letters* 11, no.3: 158-163. https://doi.org/10.1680/jgele.21.00041

Geyer, R. M. "Estudo sobre a Potencialidade de Uso das Escórias de Aciaria como Adição ao Concreto", Tese de Doutoramento, Universidade Federal do Rio Grande do Sul, 2001.

Gu, X., K. Zuo, A. Tessari, and G. Gao. 2021. "Effect of saturation on the characteristics of P-wave and S-wave propagation in nearly saturated soils using bender elements." *Soil Dynamics and Earthquake Engineering* 145: 106742. https://doi.org/10.1016/j.soildyn.2021.106742

Hatanaka, M., and T. Masuda. 2008. "Experimental study on the relationship between degree of saturation and P-wave velocity in sandy soils." *Geotechnical engineering for disaster mitigation and rehabilitation*. Springer, Berlin, pp 346–351. https://doi.org/10.1007/978-3-540-79846-0_36

Ishihara, K., H. Tsuchiya, Y. Huang, and K. Kamada. 2001. "Recent studies on liquefaction studied on sand - effect of saturation." Proc. 4th Int. Conf. Recent. Adv. Geotech. Earthq. Eng. Soil. Dyn. 1–7.

Ishihara, K., Y. Huang, and H. Tsuchiya. 1998. "Liquefaction resistance of nearly saturated sand as correlated with longitudinal wave velocity." *Poromechanics*. CRC Press, Florida, pp 583–586.

Kambole, C., P. Paige-Green, W. K. Kupolati, J. M. Ndambuki, and A. O. Adeboje. 2017. "Basic oxygen furnace slag for road pavements: A review of material characteristics and performance for effective utilization in southern Africa."

Construction and Building Materials 148: 618–631. http://dx.doi.org/10.1016/j.conbuildmat.2017.05.036

Kokusho, T. 2000. "Correlation of pore-pressure B-value with P-wave velocity and Poisson's ratio for imperfectly saturated sand or gravel." *Soils Foundations* 40: 95–102. https://doi.org/10.3208/sandf.40.4_95

Kumar, J., and B. N. Madhusudhan. 2012. "Dynamic properties of sand from dry to fully saturated states." *Géotechnique* 62: 45–54. https://doi.org/10.1680/geot.10.P.042

Marinho, F., and O. Oliveira. 2006. "The filter paper method revisited." *Geotechnical Testing Journal* 29, no. 3: 250-258. DOI:10.1520/GTJ14125

Nishio, S. 1987. "Effect of saturation on elastic wave velocities of sand and gravel." Proc. Recent. Adv. Study Engrg. Prop. Unsaturated Soil, JGS 221–224.

NTG. 2015. "SSR Standard Specification for Roadworks." Department of Infrastructure. Northern Territory Government. Australian Department of Infrastructure. ISSN 2204-8936. http://www.nt.gov.au/infrastructure/techspecs/index.shtml

Rios, S., C. Cristelo, A. Viana da Fonseca, and C. Ferreira. 2017. "Stiffness Behavior of Soil Stabilized with Alkali-Activated Fly Ash from Small to Large Strains." *International Journal of Geomechanics* 17, no. 3: 1-12. https://doi.org/10.1061/(ASCE)GM.1943-5622.0000783

Skempton, A. W. 1954. "The Pore-Pressure Coefficients A and B." *Géotechnique* 4, no.4: 143–147. https://doi.org/10.1680/geot.1954.4.4.143

Valle-Molina, C. and K. H. Stokoe, 2012. "Seismic measurements in sand specimens with varying degrees of saturation using piezoelectric transducers." *Canadian Geotechnical Journal* 49, no.6: 671–685. https://doi.org/10.1139/t2012-033

Varanasi, S. S., V. M. R. More, M. B. V. Rao, S. R. Alli, A. K. Tangudu, and D. Santanu. 2019. "Recycling Ladle Furnace Slag as Flux in Steelmaking: A Review." *Journal of Sustainable Metallurgy* 5, no.4: 449-462. https://doi.org/10.1007/s40831-019-00243-9

Viana da Fonseca, A., C. Ferreira, and M. Fahey. 2009. "A Framework Interpreting Bender Element Tests, Combining Time-Domain and Frequency-Domain Methods." *Geotechnical Testing Journal* 32, no.2. DOI:10.1520/GTJ100974

Yang, J. 2002. "Liquefaction resistance of sand in relation to P-wave velocity." *Géotechnique* 52, no.4: 295–298. https://doi.org/10.1680/geot.2002.52.4.295